Long-Wavelength Acoustic Decay in Compact Laser Flow Loops

A. K. Cousins,* W. J., Thayer,† and V. C. H. Lo‡
Spectra Technology, Inc., Bellevue, Washington

A linear theory for the asymptotic decay of acoustic disturbances in a compact pulsed laser flow loop is developed. This is the first such theory to address the phenomena in a closed finite-length flow loop, as opposed to an open or infinite-length flow loop. The linear theory agrees well with nonlinear numerical simulation results and identifies the controlling parameters and scaling relationships important to the design of compact laser flow loops.

Nomenclature

A_c = local cross-sectional area of the gas flow duct
a_0 = speed of sound
E = total (kinetic plus internal) gas energy per unit volume
h = flow channel height
h_b = muffler depth
k_n = wavenumber, $2\pi n$
L = flow loop length (circumference)
L_b = muffler length in flow direction
$\dot{m}$ = mass flux from flow channel into muffler
P = pressure in the flow channel
p = fluctuating (deviation from mean) pressure in flow channel
p_b = fluctuating (deviation from mean) pressure in muffler
R = steady-flow resistance of muffler faceplate
s = Laplace transform variable
t = time
u = fluid velocity in the x direction
x = distance, measured along flow loop
α = $\rho_0 a_0 L/(hR)$
γ = specific heat ratio of the laser gas
η = h_b/h
λ = L_b/L
ρ_0 = mean density
ρ = fluctuating (deviation from mean) density in flow channel
ρ_b = fluctuating (deviation from mean) density in muffler

Introduction

GAS lasers require highly uniform flow in order to generate laser beams of high quality. In electrically pumped lasers, flow uniformity is also required for stability of the electric discharge. The two main classes of flow nonuniformity in gas lasers are thermal and acoustic disturbances. Both types of disturbance are consequences of the rapid, localized deposition of energy into the laser cavity. Design strategies for the elimination of these disturbances involve the use of circulator fans, heat exchangers, Helmholtz-resonator acoustic attenuators, and flow nozzles and diffusers (see Fig. 1). Cassady[1] gives an extensive discussion of laser design issues and laser flow loop components. In this paper we focus on the acoustic or pressure-related disturbances in closed compact flow loops.

Highly compact flow loops are often desirable in order to minimize laser system size, weight, gas usage, and cost. This is especially true for lasers used in commercial applications, as well as for small-to-moderate power lasers intended for sensing or other mobile applications. The relative overpressures that occur in compact loops due to pulsed energy addition tend to be considerably higher than in the more conventional large-volume loops. These compact lasers commonly operate at pulse repetition frequencies of tens to hundreds of cycles per second. On these time scales, pressure disturbances have time to make multiple transits around the loop and through the acoustic attenuator.

The attenuation of the initial short-wavelength, high-amplitude disturbances is often a straightforward matter. However, the residual low-amplitude, long-wavelength modes are typically attenuated much less efficiently than the short-wavelength disturbances. This relatively slow decay can be a limiting factor in the maximum attainable pulse repetition frequency. Earlier work[4] on attenuation of acoustic disturbances in gas lasers has focused on the near-cavity, short-wavelength effects. The aim of the present study is an analysis of the long-wavelength effects present in a closed-loop system.

Laser Flow Loop Components

Figure 1 is a schematic diagram of a typical compact laser flow loop. The primary objective of the fluid-mechanical design of laser flow loops is to restore laser medium homogeneity in the laser cavity between pulses. An acoustic attenuator based on Helmholtz resonator design principles is utilized to damp the unsteady pressure disturbances. The attenuator is typically segmented in the flow direction so that it reacts locally to disturbances traveling along the flow loop and

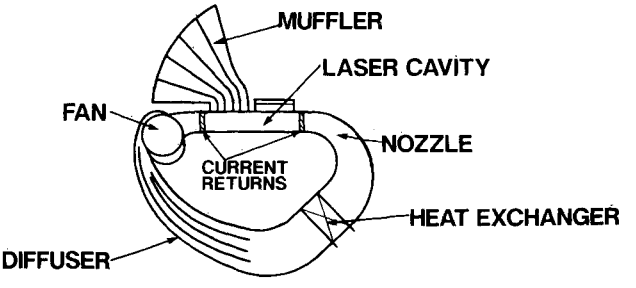

Fig. 1 Typical compact laser flow loop.

Presented as Paper 88-2746 at the AIAA Thermophysics, Plasma Dynamics and Lasers Conference, San Antonio, TX, June 27–29, 1988; received July 5, 1988; revision received Feb. 1, 1989.

*Senior Scientist, Flow Technology Group. Member AIAA.
†Technical Director, Flow Technology Group. Member AIAA.
‡Senior Scientist, Flow Technology Group.

connects with the main flow channel through a porous face plate. Clearing of the hot gas residue from the laser cavity is achieved via a mean convective flow through the laser cavity, thus necessitating the use of a circulator fan. However, because the hot gas residue travels around the loop, it will re-enter the cavity at some point and disturb the discharge; therefore, a heat exchanger is incorporated into the flow loop to remove these large-scale thermal nonuniformities. Finally, to decrease the pressure drop requirements on the circulator, a nozzle and diffuser are used to enlarge the flow channel away from the laser cavity.

The primary function of the acoustic attenuator is to damp unsteady pressure disturbances in order to restore medium homogeneity between pulses. A secondary effect of the attenuator is the redistribution of short-wavelength (comparable to the cavity size) acoustic energy into longer-wavelength, lower-amplitude disturbances that have little effect on the medium homogeneity across the laser cavity. This long-wavelength energy is eventually degraded to heat by the action of viscous processes, and removed from the loop directly by the heat exchanger as well as by conduction through the walls of the channel. An acoustically resistive muffler faceplate damps the disturbances via viscous effects, and also aids in the redistribution of acoustic energy by retarding the flow into and out of the muffler, thus spreading disturbances over longer spatial wavelengths.

The attenuator face material considered in the present study consists of a layer of fine sintered wire mesh mounted on a perforated metal backing plate. Since the flow resistance (ratio of pressure difference to velocity) of an ordinary perforated plate is proportional to the velocity through the perforations, it approaches zero for small pressure differences. However, the steady-flow resistance of the wire mesh approaches a constant as the pressure difference across the material drops to zero, and so it damps even weak pressure disturbances effectively. For this reason the wire mesh faceplate has been chosen as the most effective muffler face material for compact flow loops.

Numerical Simulation

The dynamics of the unsteady flow in the laser flow loop have been simulated numerically using the conservation equations for mass, momentum, and energy in a quasi-one-dimensional, unsteady, inviscid, compressible flow. The complexity of the multiple reflections from and interactions with the described flow loop components necessitates the use of computer modeling of the flow.

The analytical approach adopted has been to model the longitudinal unsteady phenomena in the loop as a quasi-one-dimensional ideal compressible flow. This model incorporates the effects of the cross-sectional area changes produced by the nozzle, diffuser, fan, and heat exchanger while specifically excluding from consideration multidimensional and viscous effects. The acoustic attenuator is modeled by a separate bulk model[2] that is coupled to the primary flow in the loop through the exchange of mass, momentum, and energy across the attenuator face adjacent to the flow channel.

Because of the high initial overpressures previously discussed, the fluid dynamic phenomena in a typical compact loop range from shock waves to low-amplitude acoustic disturbances. A numerical model capable of accurate representation of the flow over this dynamic range is necessary. In particular, a numerical algorithm capable of tracking shock fronts with minimal numerical dissipation and dispersion is required. At the other end of the scale, the scheme should be accurate down to disturbance levels corresponding to less than a tenth of a percent of the mean values, as medium homogeneity of this order is a typical requirement in laser flow loops. In order to meet these stringent requirements, the flux-corrected transport (FCT) scheme of Boris[3] has been utilized. This scheme handles shocklike phenomena much more accurately than other types of schemes, such as Lax-Wendroff, which can exhibit undesirable levels of numerical dissipation.

The model solves the following system of coupled conservation laws:

$$\frac{\partial}{\partial t}(\rho A_c) + \frac{\partial}{\partial x}(\rho u A_c) = s_\rho(x,t)$$

$$\frac{\partial}{\partial t}(\rho u A_c) + \frac{\partial}{\partial x}[(P + \rho u^2)A_c] = s_u(x,t)$$

$$\frac{\partial}{\partial t}(E A_c) + \frac{\partial}{\partial x}[u(P + E)A_c] = s_E(x,t)$$

$$E = P/(\gamma - 1) + \rho u^2/2$$

The nonlinear bulk muffler model previously mentioned[2] is utilized in the simulation. For the purposes of the acoustic calculation, the heat exchanger is represented by the blockage it presents to the flow and by a friction factor that gives the pressure drop through the heat exchanger as a function of the instantaneous flow Reynolds number. The fan is simulated by a combination of an area restriction and a relationship between the instantaneous pressure lift and volume flow rate through the fan.

Figure 2 shows a typical computed pressure history in the laser cavity. Three pulses are shown in the figure. The initial

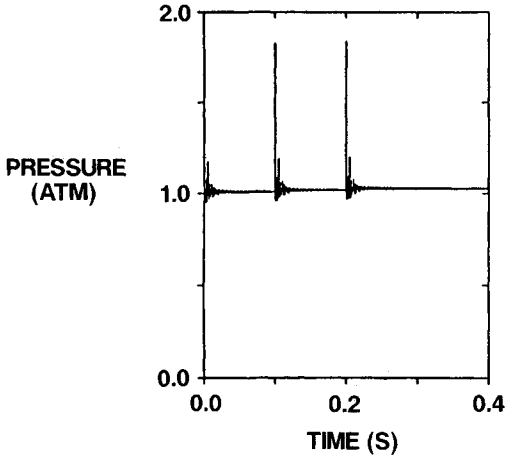

Fig. 2 Pressure history in the laser cavity.

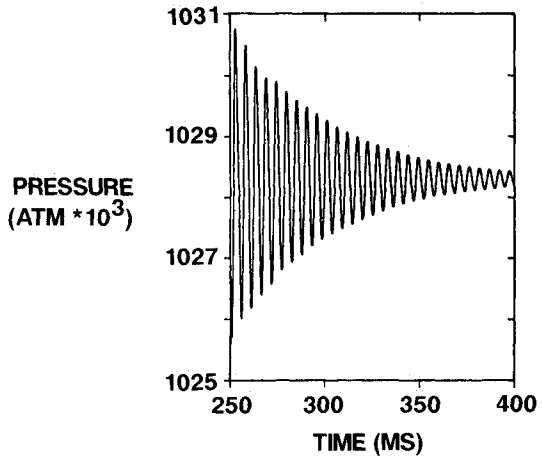

Fig. 3 Pressure history in the laser cavity.

80% overpressure is seen to decay rapidly to much lower levels as a consequence of the pressure relaxation processes and the damping effect of the acoustic attenuator. Figure 3 is a closeup of 50 ms of pressure decay (the next laser pulse would normally occur at 300 ms in this simulation). Exponential decay behavior is evident, as is a well-defined oscillation frequency (approximately 190 Hz) corresponding to the fundamental loop mode.

Figure 4 shows the logarithm of the relative pressure fluctuation ($\Delta P_{\rm rms}/\gamma P$), defined as the spatial root-mean-square of the pressure fluctuations in the laser cavity divided by the product of the mean cavity pressure and the specific heat ratio of the gas. In isentropic flow this quantity is equivalent to the relative density fluctuation of $\Delta\rho_{\rm rms}/\rho$. This particular quantity is crucial to laser discharge stability and beam quality, and typically log ($\Delta\rho_{\rm rms}/\rho$) must be kept below -3.0 or -4.0. Again, a rapid decay of fluctuations is evident, as well as the characteristic oscillation frequency. This frequency corresponds to the long-wavelength modes discussed in the introduction, i.e., modes traveling at the acoustic velocity with wavelength equal to the flow loop circumference. These modes tend to be the most difficult ones to eliminate in compact loops, and attenuating them is one of the main objectives of muffler design. The controlling muffler parameters will be derived in the linear analysis to follow.

Linear Analysis of Muffler Performance

Knight[4] has studied muffler design in the short-time regime, i.e., for lasers in which disturbances make only one transit past the muffler per pulse. We are primarily concerned here with compact flow loops, in which disturbances make a number of transits past the muffler between pulses and long-wavelength disturbances become dominant late in the pulse.

As Fig. 3 shows, after the initial highly nonlinear behavior the acoustic disturbances in a compact flow loop rapidly take the form of a well-defined decaying exponential. In this regime, characterized by relatively small fluctuation amplitudes, the decay of the long-wavelength disturbances controls the density uniformity in the laser cavity. Because of the low level of the fluctuations an attempt has been made to construct a linearized theory that predicts the asymptotic decay envelope and oscillation frequency of the pressure and density fluctuations.

It is assumed here that the acoustic disturbances are one-dimensional plane waves; cross-sectional flow area variations are neglected. Also, the mean convective velocity of the flow is neglected in comparison with the acoustic velocity; typical mean-flow Mach numbers range from 0.01 to 0.1. Finally, the acoustic impedance mismatches produced by the train of heated gas slabs from previous pulses are ignored.

With the foregoing assumptions, the linearized conservation equations are as follows:

Continuity:
$$\frac{\partial\rho}{\partial t}+\rho_0\frac{\partial u}{\partial x}=-\frac{\dot m}{h} \tag{1}$$

Momentum:
$$\rho_0\frac{\partial u}{\partial t}+\frac{\partial p}{\partial x}=0 \tag{2}$$

Entropy:
$$p=\rho a_0^2 \tag{3}$$

Note that although there is a momentum loss due to mass exchange between the flow channel and the muffler, the momentum loss term is of second order (it is proportional to the square of the velocity into the muffler) and so does not appear in the linearized momentum equation.

Taking the time derivative of the continuity equation and substituting the momentum and entropy equations into the result gives the final acoustic equation for the flow channel:

$$\frac{\partial^2\rho}{\partial t^2}-a_0^2\frac{\partial^2\rho}{\partial x^2}=-\frac{\partial}{\partial t}\left[\frac{\dot m}{h}\right] \tag{4}$$

A bulk model is used to represent the effect of the muffler:

$$\frac{\partial\rho_b(x,t)}{\partial t}=\frac{\dot m}{h_b} \tag{5a}$$

$$p_b=\rho_b a_0^2 \tag{5b}$$

An equation for the mass flux is the remaining relation required to close the set. Although the muffler face resistance has been shown to be highly nonlinear for large pressure differences, in the linear regime under consideration it is reasonable to model the resistance as a constant. Thus, the mass flux is given by

$$\dot m=\frac{\rho_0(p-p_b)}{R}=\frac{\rho_0 a_0^2}{R}(\rho-\rho_b) \tag{6}$$

If this expression for the muffler mass flux is substituted into the acoustic equation for the density in the flow channel and the resulting equation nondimensionalized by L (the flow loop length) and a_0 (the sonic speed), the result is

$$\frac{\partial^2\rho}{\partial t^2}+\alpha\left[\frac{\partial\rho}{\partial t}-\frac{\partial\rho_b}{\partial t}\right]G(x;\lambda)-\frac{\partial^2\rho}{\partial x^2}=0 \tag{7}$$

Here, $G(x;\lambda)$ is the "square wave" function defined by

$$G(x;\lambda)=\begin{cases}1, & 0\le x\le\lambda\\ 0, & \lambda\le x\le 1\end{cases}$$

The function $G(x;\lambda)$ has been introduced as a convenient representation for the finite length λ of the muffler in the flow direction; for $x>\lambda$, there is no muffler and the second term in the preceding equation vanishes.

The equation for the density fluctuation in the muffler becomes

$$\frac{\partial\rho_b}{\partial t}+(\alpha/\eta)\rho_b=(\alpha/\eta)\rho \tag{8}$$

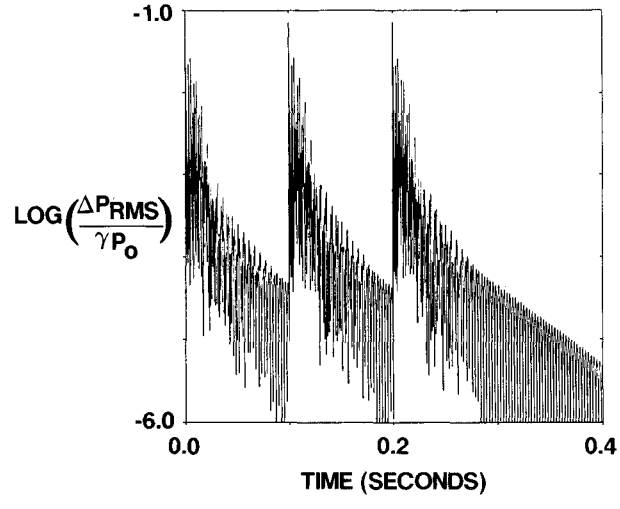

Fig. 4 Relative rms spatial pressure fluctuation in the laser cavity.

To solve Eqs. (7) and (8), we begin by taking the Laplace transforms of the equations. The Laplace transform is defined as

$$\tilde{\rho}(x,s) \equiv \int_0^\infty \rho(x,t)\, e^{-st} \mathrm{d}t$$

Assuming that the initial muffler density fluctuation is zero, the Laplace transform of Eq. (8) is

$$\tilde{\rho}_b = \frac{\alpha/\eta}{s+\alpha/\eta}\,\tilde{\rho}\, G(x;\lambda) \tag{9}$$

Here, the square wave function $G(x;\lambda)$ has again been introduced to represent the finite length of the muffler in the flow direction.

The Laplace transform of Eq. (7), utilizing Eq. (9), is

$$s^2\tilde{\rho} - s\rho(x,0) + \rho'(x,0) - \frac{\partial^2\tilde{\rho}}{\partial x^2} + \alpha\left[s\tilde{\rho} - \rho(x,0) - s\frac{\alpha/\eta}{s+\alpha/\eta}\,\tilde{\rho}\right]G(x;\lambda) = 0 \tag{10}$$

Finally, the density is expanded in a Fourier series on the interval [0,1] (since the flow loop is closed, the flow quantities are periodic on this interval):

$$\rho(x,t) = \sum_{m=-\infty}^{\infty} A_m(t)\, e^{ik_m x} \tag{11}$$

Here, $k_m \equiv 2m\pi$ and $A_{-m} = A_m^*$ since the densities are real quantities. The orthogonality property of Fourier series will also be used:

$$\int_0^1 e^{ik_m x}\, e^{-ik_n x}\, \mathrm{d}x = \delta(m-n)$$

where $\delta(m-n)$ is the Kronecker delta function. We now substitute the expansion of Eq. (11) into Eq. (10), multiply through by $e^{-ik_n x}$, and integrate from 0 to 1. The orthogonality property simplifies all terms except the last in Eq. (10), with the result

$$s^2\tilde{A}_n - sA_n(0) + A_n'(0) + k_n^2\tilde{A}_n + \alpha\sum_{p=-\infty}^{\infty}\frac{e^{ik_p\lambda}-1}{ik_p} \times\left[-A_{p+n}(0) + s\tilde{A}_{p+n} - s\frac{\alpha/\eta}{s+\alpha/\eta}\,\tilde{A}_{p+n}\right] = 0 \tag{12}$$

This equation clearly demonstrates the role of the muffler in redistributing energy among wavelengths as well as in damping the amplitudes of the individual wavelengths. Since the amplitude A_n of the nth harmonic depends on the amplitudes of all other harmonics (A_{p+n}), the muffler introduces interactions among different wavenumbers.

In the limit $\lambda \to 1$, i.e., as the length of the muffler face approaches the length of the flow loop, the exponential factor in Eq. (12) vanishes except for the $p = 0$ term; there is no interaction among wavenumbers. (Note that the limit as $p \to 0$ of the exponential term is λ).

A more interesting limit, and the one that is more closely applicable here, is $\lambda \to 0$, i.e., the limit in which the length of the muffler face in the flow direction is much smaller than the flow loop length. In the compact flow loops studied here, a typical value of λ is 0.07. For $p = 0$ in Eq. (12), the exponential term is still exactly λ; for $p \neq 0$ and $\lambda \to 0$, it is straightforward to show that this term approaches λ as well. This term can thus be factored out of the sum.

This suggests that for a particular wavenumber n, the resulting equation contains only two parameters: (α/η) and $(\alpha\lambda)$. This implies that the (dimensional) decay time τ_n of the nth harmonic depends only on these two parameters, as well as the speed of sound and the flow loop length:

$$\tau = \frac{L}{a_0} f\left[\frac{\alpha}{\eta},\ \alpha\lambda\right] \tag{13}$$

where

$$\frac{\alpha}{\eta} = \frac{\rho_0 a_0 L}{R h_b}$$

and

$$\alpha\lambda = \frac{\rho_0 a_0 L_b}{R h}$$

If more than one mode is present, the decay times will also depend on the wavenumbers of these modes through the coupling term in Eq. (12). However, the numerical evidence shows that late in the pulse, the fundamental mode ($n = 1$) is strongly dominant, and so it is reasonable to assume that the dependence on wavenumbers of other harmonics is negligible.

The form of the parameter $(\alpha\lambda)$ suggests that the muffler length scales with the height of the flow channel. Interestingly enough, it has been determined experimentally[2,4] that the same scaling exists in the short-time nonlinear regime of muffler behavior. Note also that the parameter (α/η) indicates that the muffler depth scales with the flow loop length.

Mathematically, Eq. (12) is an infinite set of linear equations in an infinite number of unknowns, so that finding a solution is not a trivial task. Rather than seeking a complete solution, it is sufficient for the present heuristic purpose to examine the dependence of the amplitude decay rates on the noted parameters.

Kantorovich and Krylov[5] discuss solution procedures for problems of this type. They show that under certain conditions, the set of equations can be solved by a series of successive approximations, i.e., by including one more wavenumber at each level of approximation, and that the approximations will converge to the exact solution. It is not difficult to show that Eq. (12) met the required conditions, but we will use a more intuitively obvious justification for restricting the set of wavenumbers considered. The numerical solution of the compact flow loop problems shows that for a large part of the pulse duration, the fundamental mode ($n = 1$) is strongly dominant. Based on this knowledge, the terms in Eq. (12) that involve interaction among modes will be dropped. The $p = 0$ term, of course, is retained; we recall that the exponential factor is equal to λ in this case. The result is

$$\tilde{A}_n\left[s^2 + k_n^2 + \alpha\lambda s - \alpha\lambda s\frac{\alpha/\eta}{s+\alpha/\eta}\right] = (s+\alpha\lambda)A_n(0) + A_n'(0) \tag{14}$$

Elementary Laplace transform inversion theory indicates that the exponential time constants for the decay of the amplitude with time are the inverses of the roots of the bracketed term, i.e., the roots of the following cubic equation in "s":

$$s^3 + \left[\frac{\alpha}{\eta} + \alpha\lambda\right]s^2 + \left[k_n^2\right]s + \left[\frac{\alpha}{\eta}\right]k_n^2 = 0 \tag{15}$$

In the limit as $\lambda \to 0$, i.e., for vanishing muffler face length in the flow direction, the roots of this equation are $-\alpha/\eta$ and $\pm ik_n$, corresponding to a decaying initial transient and a steady oscillation thereafter; in other words, a finite length of muffler is necessary to damp out the disturbances, as is intuitively obvious. Another result that should be physically obvious is that as $\alpha \to 0$, which can be achieved by making the muffler face resistance large, the roots of Eq. (15) approach 0 and $\pm ik_n$, again indicating a steady-state oscillation with no damping.

A case that may not be so obvious is the limit as $\alpha \to \infty$, which can be achieved by allowing the muffler face resistance to approach zero. In this case the roots of the characteristic equation are

$$s = \pm i\sqrt{k_n^2/(1+\lambda\eta)}$$

Thus, for zero faceplate resistance, the disturbances will oscillate steadily at a frequency somewhat smaller than their original value. The frequency shift depends on the product $(\lambda\eta)$, which represents the ratio of the muffler volume to the flow loop volume. This limiting case clearly outlines the importance of a resistive muffler faceplate in the linear disturbance regime: a muffler with a zero-resistance faceplate will redistribute energy to slightly lower frequencies but will not attenuate the disturbances. A finite resistance is necessary in order to damp disturbances.

In the limit as $(\alpha/\eta) \to 0$, corresponding to an infinite muffler depth, the roots of Eq. (15) are

$$s = 0, \quad \frac{1}{2}\left[-(\alpha\lambda) \pm \sqrt{(\alpha\lambda)^2 - 4k_n^2}\right]$$

For $\alpha\lambda \geq 2k_n$, this corresponds to a pure exponential decay; for $\alpha\lambda < 2k_n$, there is an oscillatory decay with time. The most rapid decay has a dimensionless decay time of $2/(\alpha\lambda)$.

Having examined the limiting cases of interest, further information on the amplitude decay rates can be found by solving Eq. (15) numerically. This has been done for compact flow loop parameters of interest, and the results have been compared with the full numerical solution of the nonlinear gasdynamic equations. In the cases studied here, the roots of Eq. (15) consisted of a complex conjugate pair and single negative real root. The root corresponding to the slowest decay (smallest real part) determines the decay time, while the imaginary part of the complex roots gives the frequency of oscillation. Figure 5 shows the results of this calculation for the case of the fundamental mode.

It is clear from the foregoing discussion that there should be some optimum value of muffller faceplate resistance; the two extremes of zero resistance and infinite resistance do not attenuate acoustic disturbances. In the short-time (i.e., infinite-length flow loop) limit, Knight[4,6] has also predicted the existence of an optimum value of resistance for a fixed ratio of muffler depth to flow channel height. This conclusion is verified by the FCT numerical solution. The solid curve in Fig. 5 is a plot of the dimensionless exponential decay time constant τ_1 of the fundamental mode as a function of the parameter $1/\alpha$ (which is proportional to the resistance of the muffler face). For this series of calculations, $\lambda = 0.07$ and $\eta = 6.5$. The single data points are the time constants calculated from a series of numerical simulations using the FCT code.

The first three FCT points agree remarkably well with the theory, considering the apporximate nature of the analysis. The fourth point, although qualitatively correct (i.e., indicating a minimum between the third and fourth points) and of the correct order of magnitude, deviates from the linear approximation; the reason for this deviation will be outlined. The final point to note is that the frequency of oscillation of the acoustic disturbances is predicted to within numerical error by the linear analysis; in fact, this frequency corresponds closely to the frequency of the fundamental mode.

Figure 6 shows the decay time of the nth harmonic (τ_n), normalized by the decay time of the fundamental (τ_1), as a function of n for different values of $1/\alpha$. The first four curves beginning from the bottom of the figure correspond, respectively, to the four FCT data points in Fig. 5. Note that as $1/\alpha$ increases, the decay times of the higher harmonics become commensurate with that of the fundamental mode. For the first two FCT points in Fig. 5, it is evident from Fig. 6 that the higher harmonics decay much faster than the fundamental, so that we should expect to see only the fundamental mode at late times. For the fourth FCT point in Fig. 5, Fig. 6 indicates that we should expect to find higher harmonics persisting to late times. Figures 7–10 verify these conclusions; they represent FCT pressure disturbance histories in the laser cavity and correspond, respectively, to the four data points in Fig. 5. Figures 7 and 8 show a relatively pure fundamental (although there appears to be some modulation by the first

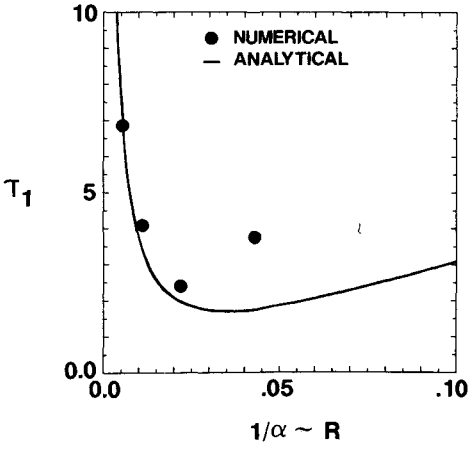

Fig. 5 Analytical and numerical predictions of the decay time constant of the fundamental mode.

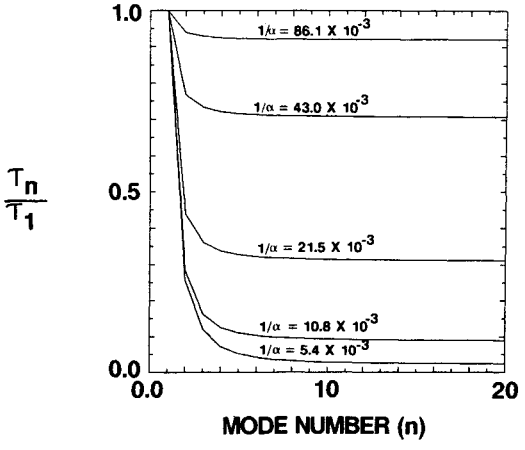

Fig. 6 Relative decay times of harmonics as a function of mode number.

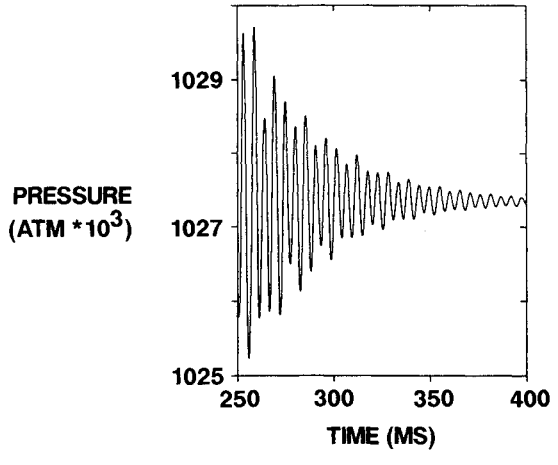

Fig. 7 Laser cavity pressure history for $1/\alpha = 5.4 \times 10^{-3}$.

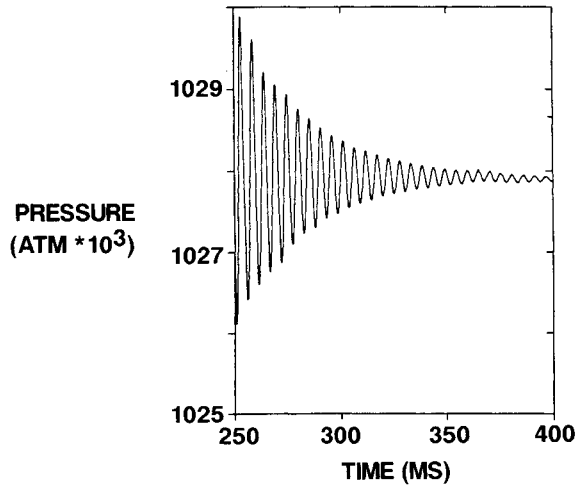

Fig. 8 Laser cavity pressure history for $1/\alpha = 10.8 \times 10^{-3}$.

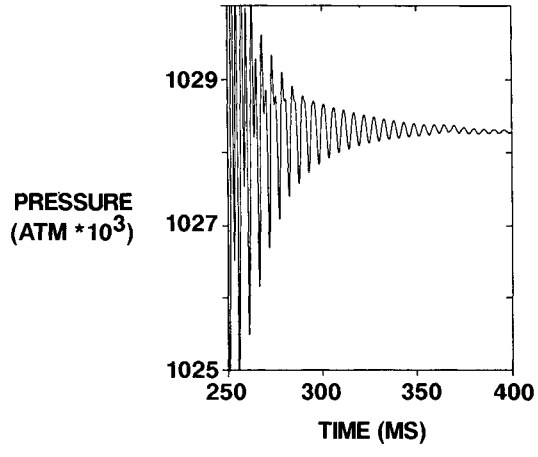

Fig. 9 Laser cavity pressure history for $1/\alpha = 21.5 \times 10^{-3}$.

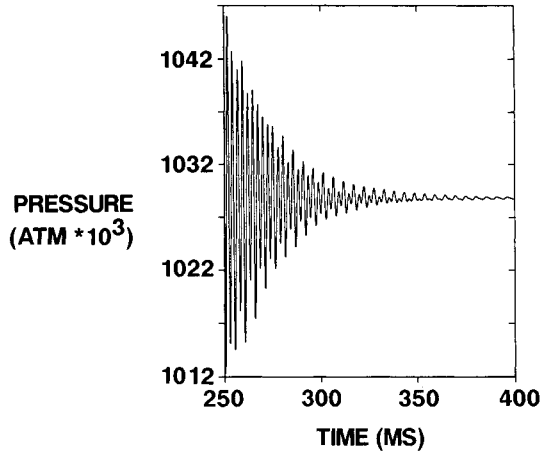

Fig. 10 Laser cavity pressure history for $1/\alpha = 43.0 \times 10^{-3}$.

subharmonic in Fig. 7); in Fig. 9, a strong first harmonic component appears initially but then decays rapidly; Fig. 10, corresponding to the fourth data point in Fig. 5, shows a strong first harmonic component persisting to late times.

The preceding considerations indicate why the approximate solution of the linear theory breaks down with increasing $1/\alpha$. It is clear that higher harmonics become more persistent as this parameter increases, so that it becomes necessary to include the mode-interaction terms in Eq. (12), which were neglected in the approximate solution. Note that $1/\alpha = 0.033$ (for the particular values of η and λ specified) corresponds to a transition point; for smaller values of $1/\alpha$, only the fundamental mode persists, while for larger values of $1/\alpha$, higher harmonics will also be present.

Knowledge of the transition to higher modes is of importance to the design of compact flow loops. In general, higher modes, with their shorter wavelengths, will contribute more strongly than the fundamental mode to gradients of density across the laser cavity. One of the primary objectives of compact flow loop design is to eliminate such gradients, and for this reason a knowledge of the parameter range in which short-wavelength disturbances persist is crucial.

Conclusions

The linear theory of disturbance decay yields a number of important insights for the design of mufflers for compact laser flow loops. The model presented here differs from earlier studies in that it includes the effects of a closed finite-length flow loop on the decay of acoustic disturbances.

The analysis identifies the parameters α, λ, and η, which control the asymptotic decay of disturbances. In the limit of small λ, i.e., muffler face length much shorter than the flow loop circumference, there are two controlling parameters, $(\alpha\lambda)$ and (α/η). In this case, the muffler depth has been shown to scale with the flow loop length and the acoustic resistance of the muffler faceplate, and the muffler length to scale with the flow channel height and the faceplate resistance.

The shortest possible decay time constant (fixing all parameters except the muffler depth) has been identified as $2/(\alpha\lambda)$ (for an infinite-depth muffler). This case constitutes an ideal limit, since in general it is necessary to utilize a finite-depth muffler in compact flow loops in order to minimize device size. For the finite-depth muffler, the existence of an optimal muffler face resistance has been determined; this optimal value of resistance has been verified by the numerical FCT simulation.

The disturbance decay time constants predicted by the linear analysis compare well with the values obtained from the full nonlinear numerical simulation. In addition, the linear theory successfully predicts the point at which the dominant asymptotic disturbance wavelength shifts from the fundamental loop mode to higher harmonics; this information is extremely useful because the higher harmonics make the largest contribution to density variations across the laser cavity.

Future analysis should extend the linear theory by including mode-interaction terms in the solution of Eq. (12). Also, although the linear predictions have been verified by nonlinear numerical studies, the ultimate test of the theory will be a comparison with experimental data taken in an operating laser flow loop.

Acknowledgments

The work presented here was supported by Spectra Technology Inc. and by MIT Lincoln Labs under Contract BX-2332.

References

[1]Cassady, P. E., "Fluid Dynamics in Closed-Cycle Pulsed Lasers," *AIAA Journal*, Vol. 23, Dec. 1985, pp. 1922–1931.

[2]Srivastava, B. N., Knight, C. J., and Zappa, O., "Acoustic Suppression in a Pulsed Laser System," AIAA Paper 79-0209, Jan. 1979.

[3]Boris, J. P., "Flux-Corrected Transport Modules for Solving Generalized Continuity Equations," Naval Research Laboratory Memorandum Rept. 3237, March 1976.

[4]Knight, C. J., "Sidewall Muffler Design for Pulsed Exciplex Lasers," *AIAA Journal*, Vol. 24, Nov. 1986, pp. 1774–1782.

[5]Kantorovich, L. V. and Krylov, V. I., *Approximate Methods of Higher Analysis*, Interscience, Chap. 1, New York, 1958.

[6]Knight, C. J., "Transverse Acoustic Waves in Pulsed Lasers," *AIAA Journal*, Vol. 20, July 1982, pp. 933–939.